7. *Scott J. F., Araujo C. A*. Ferroelectric Memories // Science. 1989. No 246. P. 1400–1405.
8. *Shimada S., Aoki T*. Stabilization of the Ferroelectric γ-Phase of KNO_3 by Doping with Na^+, Determined by the Acoustic Emission Method // Chem. Lett. 1996. V. 25. P. 393–394.
9. *Westphal M. J*. Cooperative behavior during ferroelectric transitions in KNO_3 powder. J. Appl. Phys. 1993. V. 74 P. 3131–3137.

Н. П. Саргаева, П. М. Саргаев

СИНЕРГЕТИКА СТРУКТУРНЫХ ЕДИНИЦ И ОБРАТИМЫЕ ПЕРЕХОДЫ ИДЕАЛЬНЫЙ КВАНТОВЫЙ ГАЗ — КОНДЕНСАТ ЖИДКОГО ЭТАНА

Получены квантовые волновые масс-спектры частиц жидкого этана для двух уровней энергии равновесного идеального квантового газа 1) по Эйнштейну и 2) тепловой длины волны. Спектры моделируются системами из двух и более кластеров (атомов, «резонансов» с N = 2–13 и более). Кластеры состоят из легких частиц (H, H^+) при температурах тройной точки и тяжёлых (CH_3, C_2H_6) — при более высоких. При температурах максимумов теплоёмкости (бозонных пиках) системы содержат чётное число атомов водорода. Минимумам теплоёмкости соответствуют нечётные вариабельные системы. Линейные участки температурной функции угловой характеристики структуры жидкости представлены рядами модельных систем, содержащих протонные пары при T = 97 +/–5K, частицы CH_3 при 228 +/– 5K и C_2H_6 при 274 +/– 5K.

Ключевые слова: этан, жидкая фаза, синергетика, контракция, квантовые волновые масс-спектры, модельные системы, резонансы Ефимова с N = 3–13, квантовый газ тепловой длины волны, квантовый газ по Эйнштейну, масс-спектры и экстремумы теплоёмкости; бозонные пики теплоёмкости; масс-спектры и векторы жидкости, гексагональная упаковка, пентагональная координация.

N. Sargaeva, P. Sargaev

THE SYNERGY OF STRUCTURAL UNITS AND IDEAL QUANTUM GAS — CONDENSATE REVERSIBLE TRANSITIONS OF LIQUID ETHANE

Quantum wave mass spectra of liquid ethane particles were obtained for two equilibriums ideal quantum gas energy levels: 1) by Einstein, and 2) with thermal wavelength. Spectra are modulated by systems of two or more clusters (atoms, "resonances" with N = 2–13 and higher). At triple point temperature, clusters consist of light particles (H, H^+); at higher temperatures, these consist of heavy particles (CH_3, C_2H_6). At temperatures when the heat capacity yields maximum (i. e. boson peaks) these systems consist of even number of hydrogen. Minimum heat capacity correspond to odd variable systems. Linear segments of the temperature function of liquid structure angular characteristic are represented by a series of model systems, which contain proton pairs at T = 97± 5 K, CH_3 particles at 228 ± 5 K, and C_2H_6 at 274 ± 5 K

Key words: ethane, liquid phase, synergy, contraction, quantum wave mass spectra, model systems, Efimov resonance at N = 3–13; thermal wavelength quantum gas, Einstein quantum gas, mass spectra and extremums of heat capacity; heat capacity boson peaks, mass spectra and vectors of liquid, hexagonal packing, pentagonal coordination.

In liquid and gas phases, ethane's methyl groups can undergo configurational vibrations relative to each other [2; 3; 17; 21; 25]. However, solid ethane's thermal conductivity is not asso-

ciated with the rotation of methyl groups. In this case, heat transfer is modeled by low-frequency phonons and high-frequency «diffusive» modes [3]. The solid phase structural properties are appreciably maintained also in liquid state of ethane at temperatures close to the triple point [21]. The spatial arrangements of hydrogen atoms form a compact, non-spherical shape of the ethane molecule. These features, along with not being compromised by thermal motion, are attractive factors to form proton pairing, as well as clusters of three or more atoms. Efimov substantiated the possible existence of low energy systems, consisting of three resonantly interacting particles [14; 15]. These Efimov resonances are observed in ultra-cold atoms under of low pressure vapors [18; 19; 24]. A manifestation of proton pairs has been observed in water liquid phase [5; 23]. These effects were found in the model of structural units of liquid [7; 10] and in the theory of Einstein monatomic ideal quantum gas [16]. Such findings and theories [5–10; 23] are used in this work in order to demonstrate structure and manifestations of Efimov resonances in liquid ethane.

Some concepts and definitions

We use the mass of a cluster (containing *n*, non-chemically, resonantly interacting particles) as a criterion to evaluate possible formation of Efimov resonances in liquid ethane. The cluster mass increases as particles are added to the cluster. Two or more interacting clusters constitute a system. The mass of the system is less than the mass of the light cluster. It decreases with increasing number of clusters (e. g., the same mass). For instance, in the case of H_2O [5; 23] proton pair ($2H^+$) is characterized by the reduced mass; therefore, $2H^+$ and $1O^{-2}$ particles are clusters, and the model system ($2H^+$; $1O^{-2}$) is not a classic three-body Efimov resonance. The masses of clusters and systems at different temperatures are called mass spectra.

The mass of particles is represented in atomic mass units (*u*).

Following values were used that correspond to the natural isotopic composition of hydrogen: mass of a hydrogen atom (1,00794) and mass of a proton (1,00739).

BEC and mass-spectra

The necessary conditions to facilitate appearance of a Bose-Einstein condensate (BEC) [1, p. 30], are presented in formula of the critical temperature (T_c) in the simplest form as

$$T_c = (h^2 / (2 \cdot \pi \cdot m \cdot k)) \cdot (n / 2{,}612)^{2/3}, \quad (1)$$

where *m* and *n* are molecular weight and concentration, respectively, of particles of the system (gas); *h, k* are Planck and Boltzmann constants, respectively.

In formula (1), if the molecular weight of ethane is used as *m*, along with characteristics of the liquid at the triple point (T_{trp}), we obtain the value of (T_c) 90 K below the temperature T_{trp}. Consequently, the critical temperature (T_c) may be within the range of temperatures (T, K) justifying the existence of a stable state of the liquid when the value of *m* significantly less than the molecular mass of ethane. Introducing *m* in (1) as an unknown variable, if temperatures (T_c) and (T) are considered equal and using the known factor as well as converting to atomic mass units (*u*), we obtain the following formula:

$$m(1) = 1{,}08521538\ \rho^{2/5} / T^{3/5}, \quad (2)$$

where ρ is density (in $kg \cdot m^{-3}$); m(1) has the dimension (*u*).

The values of $m(1)$ as per equation 2, correspond to the «single-atom» system. This system is not assumed to generate each atom of the molecule as independent entity. When taking into account all (N) atoms of the molecule we obtain the formula

$$m(N) = N^{8/5} \cdot m(1). \tag{3}$$

In the case of ethane $N = 8$; $m(N) = m(8) = 8^{8/5} \cdot m(1) = 27{,}857618 \cdot m(1)$.

Equations (1), (2) and (3) correspond to the critical temperature (T_c) the appearance of BEC. In this case the energy of the main part of the condensate particles is greater than zero; particles in the zero energy state are practically absent [4, p. 614]. Mass spectra of (2) and (3) describe the condensed phase, density of which is used in the calculations. The values of m(1) and m(8) (see fig. 1) from NIST [20] for the C_2H_6 liquid saturation, were used in formula (2) and (3). Similarly, for the solid ethane, the values of $m(1)_s$ and $m(8)_s$ were derived from Klimenko work [2].

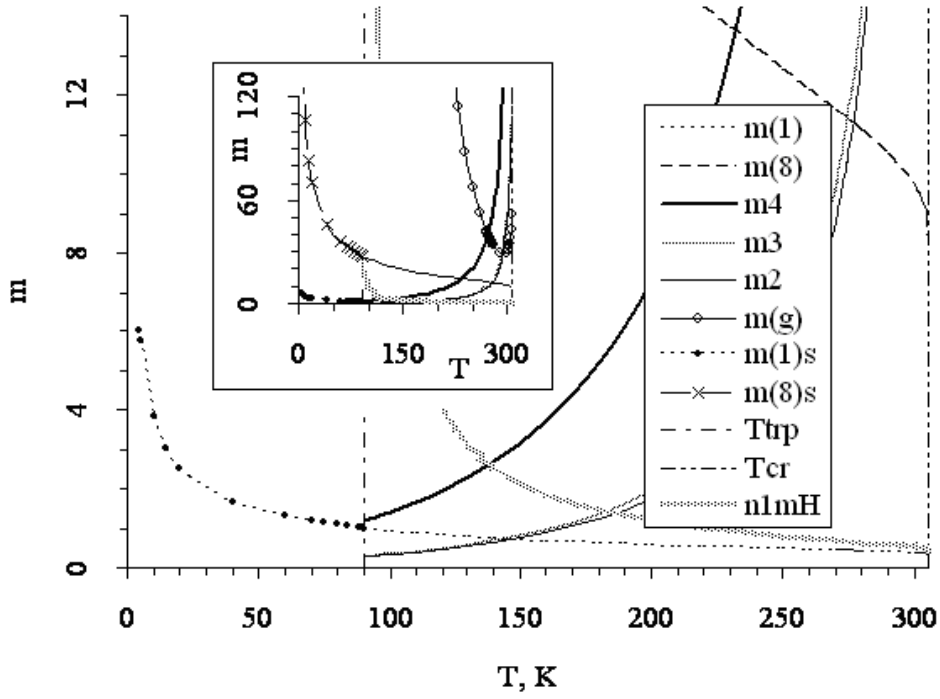

Fig. 1. The temperature dependence (T, K from equations (2 – 4)) model of the masses (m) of ethane particles at liquid saturation (m_g, m(1), m(8), m_2, m_3, m_4) and solid phase ($m(1)_s$, $m(8)_s$); structural units (m_g) of the energy levels of thermal wavelength (m_4), the equilibrium of the saturated (m_2) and fully unsaturated (m_3) of a quantum gas per Einstein [16]; of monatomic (m(1), $m(1)_s$) and 8-atom (m(8), $m(8)_s$) model of the liquid at the conditions at BEC (T_{cr}, T_{trp} — critical and triple point temperature, respectively)

The figures of $m(1)$ and $m(8)$ relate to each other via the constant coefficient in the formula (3), as the temperature relationship of these figures (fig. 1) has many common aspects: both decrease as temperature increases; the highest correlation coefficients correspond to polynomial relationship (order 16), and the trend line, when extrapolated to the low-temperature region, follows a function corresponding to the solid phase, $m(1)_s$ and $m(8)_s$.

Mass-spectra classification

This work describes the model of the resonant interaction of C_2H_6 fluid particles at different levels of energy equilibrium of the monatomic quantum gas. This modeling technique was tested using H_2O and D_2O liquid [5; 23]. According to that work, the energy ($E_c = m \cdot C^2_{зв}$) of the configurational vibrations of fluid particles (involved in the reversible transition from quantum gas to BEC), is equivalent to the vibrational energy of the particles of the quantum gas at equilibrium $E_{i.g.} = (C_p/C_v)\ k \cdot T$, where $C_{зв}$ is speed of sound in liquid; C_p/C_v — adiabatic component; C_p and C_v — Isobaric and isochoric heat capacity of quantum gas. In our work, the unknown quantity chosen is the mass of the fluid particles is computed as:

$$m = (C_p/C_v) \cdot k \cdot T / C^2_{зв}, \quad (4)$$

Similarly to the vibrational energy of the particles of the quantum gas at equilibrium, the value of *m* is dependent on the adiabatic component.

Four levels of energy [5] are used to differentiate (and to annotate) values of the mass of fluid *m* in the equation (4). These correspond to the following values of the adiabatic equilibrium of quantum gas:

$(C_p/C_v)_1 = 1$ is level (1) for a quantum gas with a critical adiabat; $(C_p/C_v)_2 = 3/2$ and $(C_p/C_v)_3 = (5/3)$ — levels of saturated (2) and fully unsaturated ($_3$) ideal monoatomic quantum gas of Einstein [16]; $(C_p/C_v)_4 = 2 \cdot \pi$ — level ($_4$) quantum gas with a thermal wavelength of particles.

The significance of m_2, m_3, m_4 for C_2H_6 liquid saturation (obtained by equation (4) using data from NIST Standard Reference Database [20]), is depicted in fig. 1. Figure 1 shows dependency of *m* on temperature (T, K).

C_2H_6 Liquid structure modeling

Additional information about the liquid structure is necessary to interpret the mass-spectra within a wide temperature range. Here, we used C_2H_6 liquid heat capacity temperature dependency at saturation (see fig. 2) and the results of an original method of vector analysis of C_2H_6 liquid structure. This vector analysis of liquid structure proposed by us in [9], supplemented [5] and tested in the case of H_2O [9], D_2O [6] and CH_4 [8] fluids.

Synergetics of the structural units is accompanied by liquid compression. During this event, the molecule on the surface of the structural units, disperse into lattices of the neighboring particles. In turn, a differentiation of molecules into two types occurs: in the «*nodes*» — type 1 and «*interstitial*» — type 2. Molecules of type 1 are characterized by fraction (part, f_1) and coordination numbers (z_1). The characteristics of the molecules of type 2 have designations f_2, z_2. Fractions are linked by equation $f_1 + f_2 = 1$. Vector sum of the coordination numbers (z_1, z_2) of two types of the molecules is equal to the coordination number of the first coordination shell (z) of the liquid molecules. In the triangle formed by vectors (z, z_1, z_2), opposite side (z_1) angle (F_1) is derived by employing the theorem of cosines. The liquid compression is related to the pressure $P_g = \sigma/(r \cdot g^{1/3})$, where σ is surface tension, *r* is radius of the molecules and *g* is the number of molecules in the structural unit. Here, the methods of assessing the number of molecules is equal to that of our previous work [8] with the only difference being that the coefficient f_{01} in ((4), [8]) was set at 1. To estimate the coefficient f_{01}, g was derived at the triple point of ethane (g = 413) employing previously described technique [10] from the densities of solid and liquid phases of ethane [2; 13; 20; 25]. As temperature increases, the number of molecules in the structural units

of ethane passes through a minimum at 290–300 K. The mass of structural units (m_g), corresponding to the temperature minimum of g, are shown in fig. 1.

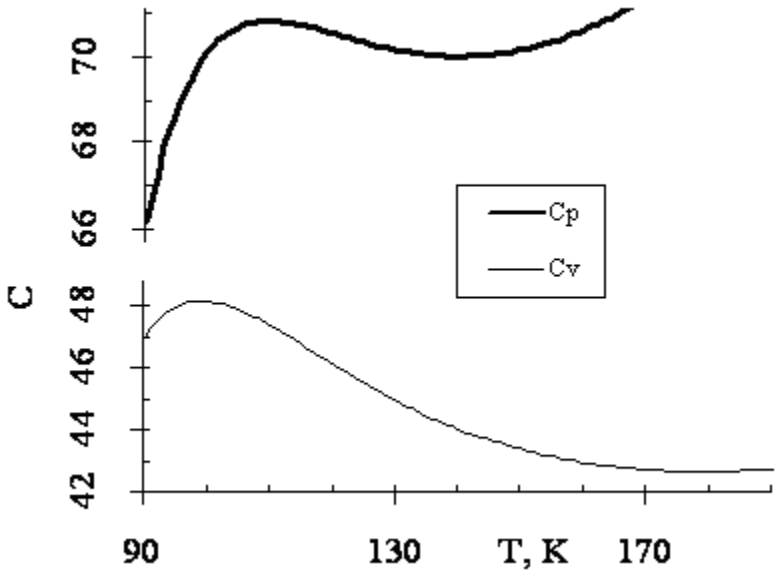

Fig. 2. Isobaric (C_p) and isochoric (C_v) heat capacities (C, J·mol^{-1}) at the C_2H_6 fluid saturation according to NIST Standard Reference Database [20] at temperatures (T, K)

The biggest difference in structures of ethane and methane [8] at liquid saturation point are evident in the temperature dependence of angles characteristics. In the case of ethane, the trend line (F_1 (T)) the angle of the opposite side of the z_1, has linear and non-linear segments. Linear plots correspond to high values of correlation coefficient (r^2). Fig. 3 shows the values of r^2 as deviations from 1 ($Y = (1 - r^2)\cdot 10^4$) for the function (F_1 (T)). Coefficient (r^2) was evaluated across 50 points. F_1 was determined after every 0.2 K. Therefore, 10K temperature intervals are shown in Fig. 3 (with the exception of point 2, where the interval is 0,2 K). For all cases, a linear function $F_1 = A_0 + A_1\cdot T$ was obtained when determining the correlation coefficient (r^2). Here, the coefficients (A_0, A_1) are temperature dependent. The function (A_0 (T)) is shown in fig. 4.

To interpret the mass-spectra obtained in this work, the numerical values of the masses were associated with the thermal capacity extremes and angular characteristics of the structure. Figure 2 shows that in the case of ethane at liquid saturation, there are two temperatures corresponding to the maximum and two corresponding to the minimum heat capacity of liquid. The maxima are adjacent to the triple point and the minima are located in the higher-temperature region. The furthest from the triple point temperature minimum is described as C_v (T). With further increase in temperature, both C_p and C_v increase.

The maximum values of the correlation coefficient r^2, shown in fig. 3 correspond to Y = 0, which are periodically repeat as temperature increases. The first maximum (r^2) is adjacent to the temperature of the triple point, similarly to the maxima of the heat capacity. Second and third maxima are observed at 228 K and 274,2 K.

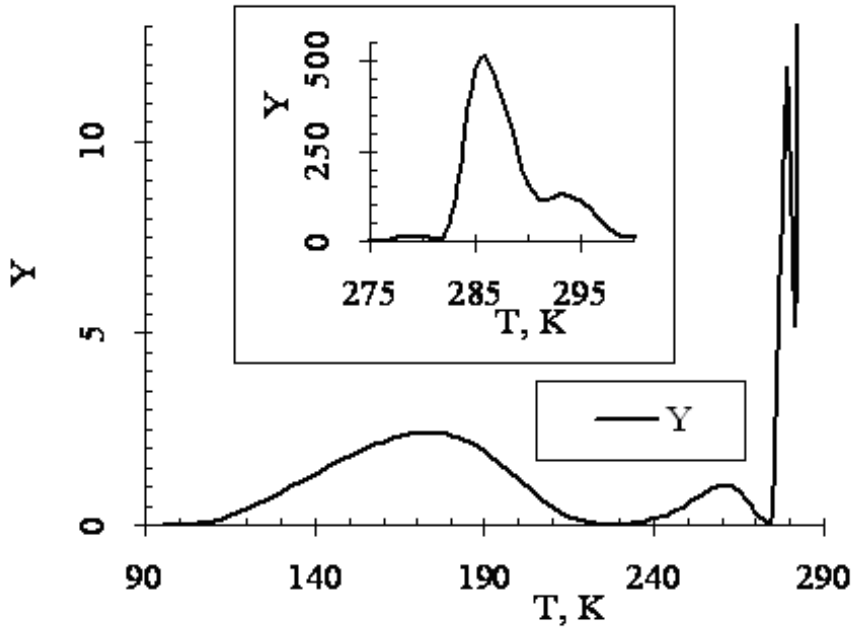

Fig. 3. The correlation coefficient (r^2), presented as a deviation from the norm $(1–r^2)\cdot10^4$, (Y) a linear function of the angle ($F_1(T)$), the opposite side of the vector z_1 of coordination numbers z, z_1 and z_2 of ethane at fluid saturation depending on the temperature (T, K)

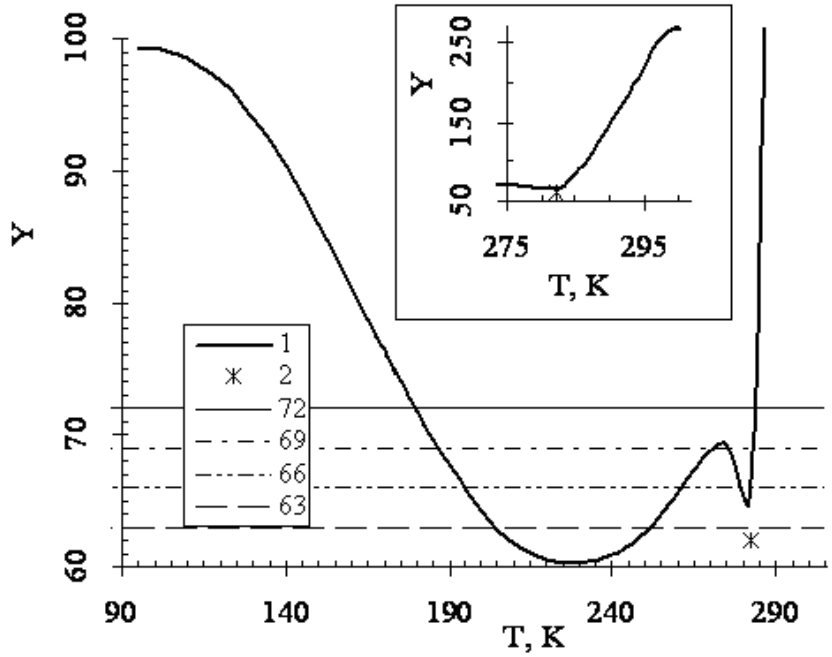

Fig. 4. The coefficient A_0 (Y, degree) of a linear equation of the temperature dependence on the angle $F_1(T)$, of the opposite side of the triangle of vectors z_1 coordination numbers z, z_1, z_2 C_2H_6-liquid saturation as a function of temperature (T, K): 50 points in the temperature range 10 K (1) and two points in the range 0,2 K (2) were used to generate the plot; 72 — angle, the characteristic pentagonal orientation; 63, 66 and 69° angles fall in the range of 60° to 72°

Temperature range of the first minimum (r^2) is wider than that of the second, to the point that is practically overlaps with the temperature of *minimum* C_v *heat capacity* of the liquid. The structural differences of the liquid ethane are best illustrated in figure 4. In the Figure, the coefficient A_0 describes the structure that is formed from the molecule type 1 during the cooling of the liquid molecules located at the lattices. At temperatures that correspond to maxima of r^2 (T), the system tends to form a hexagonal orientation with typical 60° angles. Temperature minimum r^2 (T) is better described pentagonal coordination with typical 72° angles.

Structure with a typical 100^o degree angle is formed when the liquid is cooled near the triple point. This value corresponds to the mean of the characteristic angles (90^o and 109^o) body-centered cubic lattice, which is found in the solid phase at temperatures near the triple point of ethane [2; 12; 25].

The mass spectra intersection and overlapping

The m(1) trendline and the m_3(T) curve (Figure 1), corresponding to the utmost unsaturated quantum Einstein gas [16], cross at the temperature of 139 K. This temperature is equal to that of the isobaric heat capacity C_p(T) minimum (fig. 2). The m(1) and the m_2(T) spectra cross at 145 K, where the C_p(T) values start to increase. Nonetheless, at the isochoric heat capacity temperature minimum the m(1) and m_2 relate as follows m2 = 2 * m(1) (detailed information can be found in the section «mass spectra and C_p(T) and C_v(T) function minima»). The m(1) values could be also obtained as reduced masses of the two body system (1H; n1mH), where 1H corresponds to the mass of hydrogen atom, and the n1mH(T) mass spectrum possesses three remarkable intersections (Figure 1). At the triple temperature point the n1mH value is equal to that of the m(8) (the first intersection). Then the n1mH values abruptly fall with the temperature increase. The n1mH experiences the second intersection with the m_4(T) curve and the third one with the m_3(T) and m_2(T) curves when the temperature drop is less abrupt. The second and the third intersections correspond to the heat capacity temperature minima (Figure 2), where the low-temperature intersection matches the isobaric heat capacity Cp(T) temperature minimum, and that of the high-temperature matches the isochoric heat capacity Cv(T) temperature minimum.

While the m(1) and the m(8) are falling with the temperature increase, the m_2, m_3, m_4 are rising up. These get multiplied by 379 times in orthobaric conditions when the temperature increases from the triple point of 90.352 K up to the critical point of 305.33 K. The m(8) trendline crosses the m_4(T) at 230 K as well as the m_3(T) and the m_2(T) curves at 274 K (Figure 1). Both temperatures are equal to those of the temperature maxima of the correlation coefficient r^2, which is shown in figure 3. These maxima, in turn, correspond to the most linear segments of the temperature dependence F_1(T) of an angle opposite to the z_1 side of the triangle. Where the triangle is formed by the z, z_1, and z_2 vectors of the C_2H_6 liquid coordination numbers (on the saturation line).

Mass spectra and the boson nature of heat capacity maxima

The reasons for the mass spectra related appearance of heat capacity (and other functions) extremums should initiate from the model system properties since extremum values are not present in mass spectra themselves as follows from the Figure 1. At the temperature range from the triple point to 122 K the mass of particles with thermal wavelength (m_4) is less than 2. It can be modeled as a reduced mass of the system with two or more clusters. In such system the light cluster contains two protons (or 2 hydrogen atoms) and is called the «*2H-system»*. The appearance of

proton pairs in the heat capacity of C_2H_6-liquid determined in this research is in agreement with the results for water [5; 23]. However, there are differences between the two compared factors: the H_2O proton pairs occur on the energy level of Einstein quantum gas, while in case of the C_2H_6-liquid they occur on the quantum gas energy level with the thermal wavelength. Yet, this difference does not change the quantum nature of the proton pair — in either case it is associated with the class of bosons. In this regard, the C_2H_6-liquid heat capacity maximum at the temperature of 99 K can be viewed as a «*boson peak*».

The boson contribution into the heat capacity $C_v(T)$ is further supported by the increased *parity of the model system* when the temperature increases and approaches the $C_v(T)$ maximum in the low-temperature extreme. At the triple point the model system has an *even-odd* composition (2H; 3H), and in the close proximity to the $C_v(T)$ maximum it has an *even-even* composition (2H; 4H). The (2H; 4H) system is a *critical even-even system*. The following (2H; 6H) system has some «probability irrelevance» as the sum of the hydrogen atom number exceeds its number in the two methyl groups which could be the reason for the heat capacity decrease. There are no such problems in the equivalent (3H; 3H) system, but there are quantum reasons for the possible heat capacity decrease of this liquid. The 3H clusters contain an odd number of hydrogen atoms or protons. In the case of protons (which is more realistic due to the difference in the electronegativity of hydrogen and carbon atoms), the 3H clusters (or some of them) can be classified as fermions. The fermion interference leads to a decrease of the particle oscillation amplitude [11, p. 31], which could be the reason for the attenuation of particle oscillation and the decrease of the liquid heat capacity.

The decline of the isochoric heat capacity with the temperature increase is very fast and is strongly influencing the temperature trend of the isobaric heat capacity $C_p(T)$ of liquid. Above 109.7 K the $C_p(T)$, similar to $C_v(T)$, starts lowering down with the following temperature increase. At 109,7 K the m_4 = 1,6381 value is modulated by the (2H; 10H; 2M), system, where *the sum of hydrogen atoms* (in the clusters of 2H and 10H) is equal to 12. This corresponds to the *two ethane molecules*. With further increase of hydrogen atom number in the *even-even* system the probability problems rise up. These problems are associated with the *coherent movement* of the atoms of the third molecule, i.e. the system become critical. In the regions of $C_v(T)$ and $C_p(T)$ maxima the model systems of m_4-spectrum are *similar* and can be characterized as *even-even hydrogen-critical* systems (on the monomolecular levels for C_v and on the bimolecular levels for C_p). This proves the *boson nature* of the heat capacity *maxima* for the C_2H_6- liquid on the saturation line.

Mass-spectra and the nature of C_p (T) and C_v (T) minima

At a temperature of 178,6 K, which according to NIST Standard Reference Database [20] is close to $C_v(T)$, the m_2 value (1,2073) is twice of that of m(1) (0,6039). Note, that the m_4 value corresponds to the mass of *five hydrogen atoms* that can be obtained as the reduced mass of the two clusters. The mass of the first of which is equal to the mass of the *six hydrogen atoms (protons)* and the second to the mass of one ethane molecule (6H; 1M).

Manifestation of hexatomic «Efimov resonance» (6H), like *10-atom* (10H), in itself, is important for quantum mechanics phenomenon. But equally important is the fact that adding another cluster (1M) to (6H; 1M) system, causes *decoherence* of the 6H cluster and increases the *variability* of the model system. The reduced mass of the model system, followed by variations in composition, abruptly reaches m_3 at temperatures corresponding to the minimum isochoric heat capacity of liquid ethane. For example, the *odd-odd* system (3H; 3H; 1M; 1M) (or (3H; 3H;

1CH3)) corresponds to the values of the reduced mass of 1,3731 to 1,3738. The lower limit is employed in calculating of the mass of a proton, the upper — the mass of a hydrogen atom. Both results correspond to values of m_3 of the temperature minimum of $C_V(T)$, while increasing the number of clusters with a mass of ethane molecules in a model system — shifting to the trend line $m_2(T)$ in this temperature range. At the limit, when $m_2(T)$ values reach mass-spectrum in the temperature associated with minimum isochoric heat capacity of liquid, the model system contains two clusters of type 3H and five of 1M. In this case, the reduced mass of the five clusters 1M (6,0138) is close to half the atomic weight of carbon, and the model system can be replaced by an equivalent (3H; 3H; 1C; 1C), in which the *total mass* of the cluster is equal to that of a molecular mass of ethane. In a different case, where a model system (3H; 3H; 1C; 1C), 3H clusters are composed of protons and clusters 1C consisting of carbon atoms with a net charge of –3, the reduced mass is equal to 1,20733, which is equal to that of the m_2 at a temperature of 178,6 K. 50% of the obtained m_2 value (0,60367), is equal to that of m(1) at the same temperature. Consequently, at a minimum isochoric heat capacity of fluid saturation mass m_2 (of the *condensate particles* involved in the *reversible transitions* in the *equilibrium saturated monatomic ideal quantum gas by Einstein)*, can be found as the reduced mass of the model system (3H; 3H; 1C; 1C). At the same temperature under conditions leading to BEC, particle mass m(1), calculated by equation (2), can be obtained as the reduced mass of the *two model systems* of the same composition as for the m_2 (3H; 3H; 1C; 1C).

Hydrogen oddness and *variability* of model systems at temperatures of C_v *minimum*, which are discussed in detail above, are the main properties of model systems in the field of *temperature minimum of the isobaric heat capacity* of liquid (139,8 K). For example, with m_4 = 2,6848 in these conditions corresponds to the following model systems: (3H; 1M-6H), (4H; 8H), (5H; 7H; 1M), ((6H; 6H) ≡ 3H; 1M-6H). Manifestation of systems *without «hydrogen» content clusters* (at temperatures corresponding to the minimum heat capacity of liquid and higher, $C_p(T)$ и $C_v(T)$) characterizes the system as a model *variable*.

At constant temperature, m_2, m_3 and m_4, demonstrate constant relations indicating adiabat with an average value of m_2 and m_3 almost 4 times less than the m_4. Consequently, the discovered mechanism for conversion of mass-spectra $m_4(T) \leftrightarrow m_3(T)$ and $m_4(T) \leftrightarrow m_2(T)$, which is based on a modification of the model system and which corresponds to the temperature $C_V(T)$ minimum, has universal character.

Mass-spectra and structure of liquid

Model systems of the m_4 mass spectrum that correspond to the r^2 temperature maxima could be compared using three points, the two of which are located +/–5 K from the r^2 maximum as the later one was defined within the 10 K region. At 228 +/– 5K such a comparison results in the row of ($1CH_3$; $3CH_3$), ($1CH_3$; $5CH_3$), ($1CH_3$; $13CH_3$), which *repeats* at 274,2 +/– 5K (2M; 3M), (2M; 5M), (2M; 13M), and 96,6 +/– 5 K — (1,5H; 3(2H)), (1,5H; 5(2H)), (1,5H; 13(2H)). In the latter case the series of second clusters consist of the proton pairs classified as bosons; while the first cluster can be defined as equivalent (2H; 6H) and (3H; 3H) systems. These systems, as was noted previously, are not equivalent in terms of the quantum mechanics: in the first case (2H; 6H) boson properties are dominated, when in the second case (3H; 3H) fermion properties are dominated.

Quantum wave mass spectra of liquid ethane particles, which correspond to the energy levels of a quantum gas particles according to Einstein and to the thermal wavelength, can be modulated by the system of two and more clusters (or atoms, «resonances» with N = 2–13 or higher)

predominantly composed of hydrogen at the triple point temperature and of heavier particles (CH_3, C_2H_6) at higher temperatures.

The boson nature of the maximum of ethane heat capacity can be characterized by the model systems of even hydrogen atom numbers at heat capacity temperature maxima; on the other hand it can be characterized by the odd variables at regions of minima of liquid heat capacity. Linear segments of angular characteristic temperature functions of the liquid structure can be interpreted by the series of model systems, which contain proton pairs at the temperature of 97 K CH_3 particles at 228 K, and C_2H_6 particles at 274 K.

СПИСОК ЛИТЕРАТУРЫ

1. *Гриншейн Дж., Зайонц А.* Квантовый вызов // Современные исследования оснований квантовой механики. Долгопрудный: Интеллект, 2008. 400 с.

2. *Клименко Н. А., Гальцов Н. Н., Прохватилов А. И.* Структура, фазовые переходы и тепловое расширение этана C_2H_6 // Физика низких температур. 2008. Т. 34. № 12. С. 1319–1326.

3. *Константинов В. А., Ревякин В. П., Саган В. В.* Вращение метильных групп и теплопроводность молекулярных кристаллов: этан // Физика низких температур. 2006. Т. 32. № 7. С. 905–912.

4. *Левич В. Г., Вдовин Ю. А., Мямлин В. А.* Курс теоретической физики. М.: Наука, 1971. Т. 2. 936 с.

5. *Саргаева Н. П., Барышев А. Н., Саргаев П. М.* Бозоно-фермионные контрасты синергетики структурных единиц жидких D_2O и H_2O // Известия РГПУ им. А. И. Герцена. 2009. № 95. С. 120–133.

6. *Саргаева Н. П., Наймушин А. Б., Саргаев П. М.* Синергетика структурных единиц и термодинамические свойства D_2O жидкости // Известия РГПУ им. А. И. Герцена. 2008. № 9(48). С. 44–60.

7. *Саргаева Н. П., Саргаев П. М.* Кластеры — суть структуры жидкого состояния воды // Известия РГПУ им. А. И. Герцена. 2007. № 7(26). С. 112–126.

8. *Саргаева Н. П., Саргаев П. М.* Синергетика структурных единиц и равновесие двух типов молекул жидкого метана // Известия РГПУ им. А. И. Герцена. 2010. № 122. С. 73–84.

9. *Саргаева Н. П., Саргаев П. М.* Координационно-угловое распределение молекул воды в растворах // Всероссийский симпозиум «Эффекты среды и процессы комплексообразования в растворах»: Тезисы докладов. Красноярск, 2006. С.193–194.

10. *Саргаев П. М.* Проявление структуры воды в электрофизических свойствах биосистем и методы мониторинга: Автореф. дис. ... д-ра хим. наук. СПб., 1999. 39 с.

11. *Фейнман Р., Лейтон Р., Сэндс Р.* Фейнмановские лекции. М.: Мир. 1978. Вып. 8, 9. 528 с.

12. *Amoureux J. P., Foulon M., Muller M.* and *Bee M.* Structures of Ethane, Hexamethylethane and Hexamethyldisilane in theirPlastic Phases // Acta Crystallography. 1986. Vol. B42. P. 78–84.

13. *Atake T., Chihara H.* Calorimetric study of the phase changes in solid ethane // Chem. Lett. 1976. № 7. P. 683–688.

14. *Efimov V.* Energy Levels Arising from Resonant Two-Body Forces in a Three-Body System // Phys. Lett. 1970. Vol. B33. № 8. P. 563–564.

15. *Efimov V.* Low-Energy Properties of Three Resonantly Interacting Particles // Sov. J. Nucl. Phys. 1979. Vol. 29(4), April. 546–553.

16. Einstein A. Quantentheorie des einatomigen idealen Gases // Sitzungsber. preuss. Akad. Wiss., Phys.-math. K1. 1925. S. 3–14.

17. *Kemp J. D., Pitzer K. S.* The Entropy of Ethane and the Third Law of Thermodynamics. Hindered Rotation of Methyl Groups // J. Am. Chem. Soc. 1937. Vol. 59. № 2. P. 276–279.

18. *Knoop S., Ferlaino F., Mark M., Berninger M., Schöbel H., Nägerl H.-C., Grimm R.* Observation of an Efimov-like trimer resonance in ultracold atom–dimer scattering // arXiv:0807.3306v1 [cond-mat.other] 21 Jul 2008. 12 p.

19. *Kraemer T., Mark M., Waldburger P., Danzl J. G., Chin C., Engeser B., Lange A. D., Pilch K., Jaakkola A., Nägerl H.-C.* and *Grimm R.* Evidence for Efimov quantum states in an ultracold gas of caesium atoms // Nature. 2006. Vol. 440. 16 March. P. 315–318.

20. NIST Standard Reference Database Number 69, June 2005 Release.

21. *Pursky O. I., Sysoev V. M*. Thermal conductivity of simple molecular substances at crystal-liquid phase transition // Bulletin of University of Kyiv Series: Physics & Mathematics. 2009. Vol. 2. 6 p.

22. *Sargaeva N. P., Baryshev A. N., Puchkov L. V., Sargaev P. M*. The speed of sound and water structural units // XVII International Conference on Chemical Thermodynamics in Russia. Abstracts. Vol. 1. Kazan, Russian Federation. June 29 – July 3. 2009. P. 210.

23. *Sargaeva N. P., Baryshev A. N., Puchkov L. V., Sargaev P. M*. Heat capacity bose-fermi contrasts of D_2O and H_2O liquids // XVII International Conference on Chemical Thermodynamics in Russia. Abstracts. Vol. 1. Kazan, Russian Federation. June 29 – July 3. 2009. P. 210.

24. *Wang X. P.* On the existence of the N-body Efimov effect // J. Funct. Analysis. 2004. Vol. 209. P. 137–161.

25. *Younglove B. A., Ely J. F.* Thermophysical properties of fluids. II. Methane, ethane, propane, isobutane and normal butane // J. Phys. Chem. Ref. Data. 1987. Vol. 16. P. 577–798.

REFERENCES

1. *Grinshtejn Dzh., Zajonc A*. Kvantovyj vyzov. Sovremennye issledovanija osnovanij kvantovoj mehaniki. Dolgoprudnyj: Intellekt. 2008. 400 s.

2. *Klimenko N. A., Gal'cov N. N., Prohvatilov A. I*. Struktura, fazovye perehody i teplovoe rasshirenie jetana S2N6 // Fizika nizkih temperatur. 2008. T. 34. № 12. S. 1319–1326.

3. *Konstantinov V. A., Revjakin V. P., Sagan V. V*. Vrawenie metil'nyh grupp i teploprovodnost' molekuljarnyh kristallov: jetan // Fizika nizkih temperatur. 2006. T. 32. № 7. C. 905–912.

4. *Levich V. G., Vdovin JU. A., Mjamlin V. A*. Kurs teoreticheskoj fiziki. M.: Nauka, 1971. T. 2. 936 s.

5. *Sargaeva N. P., Baryshev A. N., Sargaev P. M*. Bozono-fermionnye kontrasty sinergetiki strukturnyh edinic zhidkih $D2_O$ i $H2_O$ // Izvestija RGPU im. A. I. Gercena. 2009. № 95. C. 120–133.

6. *Sargaeva N. P., Najmushin A. B., Sargaev P. M*. Sinergetika strukturnyh edinic i termodinamicheskie svojstva D2O zhidkosti // Izvestija RGPU im. A. I. Gercen. 2008. № 9(48). C. 44–60.

7. *Sargaeva N. P., Sargaev P. M*. Klastery — sut' struktury zhidkogo sostojanija vody // Izvestija RGPU im. A. I. Gercena. 2007. № 7(26). S. 112–126.

8. *Sargaeva N. P., Sargaev P. M*. Sinergetika strukturnyh edinic i ravnovesie dvuh tipov molekul zhidkogo metana // Izvestija RGPU im. A.I. Gercena. 2010. № 122. S. 73–84.

9. *Sargaeva N. P., Sargaev P. M*. Koordinacionno-uglovoe raspredelenie molekul vody v rastvorah // Vserossijskij simpozium «JEffekty sredy i processy kompleksoobrazovanija v rastvorah»: Tezisy dokladov. Krasnojarsk. 2006. S. 193–194.

10. *Sargaev P. M*. Projavlenie struktury vody v jelektrofizicheskih svojstvah biosistem i metody monitoringa: Avtoref. dis. ... d-ra him. nauk. SPb., 1999. 39 s.

11. *Fejnman R., Lejton R., Sjends R*. Fejnmanovskie lekcii. M.: Mir, 1978. Vyp. 8, 9. 528 s.

12. *Amoureux J. P., Foulon M., Muller M*. and *Bee M.* Structures of Ethane, Hexamethylethane and Hexamethyldisilane in theirPlastic Phases // Acta Crystallography. 1986. Vol. B42. P. 78–84.

13. *Atake T., Chihara H.* Calorimetric study of the phase changes in solid ethane // Chem. Lett. 1976. № 7. P. 683–688.

14. *Efimov V*. Energy Levels Arising from Resonant Two-Body Forces in a Three-Body System // Phys. Lett. 1970. Vol. B33. № 8. P. 563–564.

15. *Efimov V*. Low-Energy Properties of Three Resonantly Interacting Particles // Sov. J. Nucl. Phys. 1979. Vol. 29(4), April. 546–553

16. *Einstein A*. Quantentheorie des einatomigen idealen Gases // Sitzungsber. preuss. Akad. Wiss., Phys.-math. K1. 1925. S. 3–14.

17. *Kemp J. D., Pitzer K. S.* The Entropy of Ethane and the Third Law of Thermodynamics. Hindered Rotation of Methyl Groups // J. Am. Chem. Soc. 1937. Vol. 59. № 2. p. 276–279.

18. *Knoop S., Ferlaino F., Mark M., Berninger M., Schöbel H., Nägerl H.-C., Grimm R.* Observation of an Efimov-like trimer resonance in ultracold atom–dimer scattering // arXiv:0807.3306v1 [cond-mat.other] 21 Jul 2008. 12 p.

19. *Kraemer T., Mark M., Waldburger P., Danzl J. G., Chin C., Engeser B., Lange A. D., Pilch K., Jaakkola A., Nägerl H.-C.* and *Grimm R*. Evidence for Efimov quantum states in an ultracold gas of caesium atoms // Nature. 2006. Vol. 440. 16 March. P. 315–318.

20. NIST Standard Reference Database Number 69, June 2005 Release.

21. *Pursky O. I., Sysoev V. M*. Thermal conductivity of simple molecular substances at crystal-liquid phase transition // Bulletin of University of Kyiv Series: Physics & Mathematics. 2009. Vol. 2. 6 p.

22. *Sargaeva N. P., Baryshev A. N., Puchkov L. V., Sargaev P. M.* The speed of sound and water structural units // XVII International Conference on Chemical Thermodynamics in Russia. Abstracts. Vol. 1. Kazan, Russian Federation. June 29 – July 3. 2009. P. 210.

23. *Sargaeva N. P., Baryshev A. N., Puchkov L. V., Sargaev P. M*. Heat capacity bose-fermi contrasts of D_2O and H_2O liquids // XVII International Conference on Chemical Thermodynamics in Russia. Abstracts. Vol. 1. Kazan, Russian Federation. June 29 – July 3. 2009. P. 210.

24. *Wang X. P.* On the existence of the N-body Efimov effect // J. Funct. Analysis. 2004. Vol. 209. p. 137–161.

25. *Younglove B. A., Ely J. F.* Thermophysical properties of fluids. II. Methane, ethane, propane, isobutane and normal butane // J. Phys. Chem. Ref. Data. 1987. Vol. 16. P. 577–798.